

Electrochemical Study of Interaction between Imidazole-Based-Ionic-Liquid and Light Petroleum in Oil/Water Emulsion

E.E. Villalobos-Neri¹, U. Páramo-García^{1,*}, R. Mayen-Mondragon^{2,*}, N.V. Gallardo-Rivas¹

¹ Tecnológico Nacional de México/I. T. Cd. Madero, Centro de Investigación en Petroquímica, Prol. Bahía de Aldhair y Av. de las Bahías, Parque de la Pequeña y Mediana Industria, 89600, Altamira, Tamaulipas, MÉXICO

² Polo Universitario de Tecnología Avanzada, Facultad de Química, Universidad Nacional Autónoma de México, Vía de la Innovación 410, Autopista MTY-Aeropuerto Km. 10, Parque PIIT, 66629, Apodaca, Nuevo León, MÉXICO.

*E-mail: uparamo@itcm.edu.mx; rmayen@unam.mx

Received: 10 February 2021 / Accepted: 15 April 2021 / Published: 30 April 2021

In the present work, the binding capacity of a 1-methyl-3-hexylimidazolium p-toluenesulfonate ionic liquid to Aragon light oil within a 70/30 oil/water emulsion was studied by cyclic voltammetry. The imidazole-based ionic liquid was synthesized by anion interchange reaction. Its chemical structure was confirmed by Fourier-Transform Infrared Spectroscopy and Nuclear Magnetic Resonance. Its Critical Micelle Concentration (CMC) in water was determined by Conductimetry, Ultraviolet-Visible Spectroscopy and Cyclic Voltammetry. The ionic-liquid-to-oil binding-constant and binding-free-energy were determined from the dependence of the voltammogram anodic-peak-current with the ionic liquid concentration in the emulsion. The diffusion coefficient of the free and bound forms of the oil within the emulsion were determined from the Randles-Sevcik equation. The measurements led to a CMC value of approximately 152 mg/L and a binding constant of $0.98 \times 10^4 \text{ M}^{-1}$, corresponding to a binding free energy of -22.78 KJ/mol. The negative value of the latter confirmed the ionic liquid spontaneously binds to the oil phase. The oil-droplets diffusion coefficient showed a 2.5-fold increase (up to $4.631 \times 10^{-7} \text{ cm}^2/\text{s}$) due to incorporation of the ionic liquid molecules. The information gathered can be helpful to design more efficient remediation processes of oil-contaminated water, as well as to improve the design of ionic liquid molecules, and to study their interaction with different oil components.

Keywords: Imidazole, diffusion coefficient, oil/water emulsion, critical micelle concentration, oil-contaminated waters

1. INTRODUCTION

The hydrocarbon industry has grown extensively during the last decades, leading unfortunately to a large number of accidents and thus to increased levels of pollution within water bodies located

around extraction, transportation or storage sites. Such pollution causes irreversible damage to plants and animals within the aforementioned environments. For example, when hydrocarbons are released into superficial water bodies, the oil phase floats due to its lower density. In this way, it blocks the passage of light and the interchange of gases, hindering the development of photosynthesis. It also allows the solubilization of materials which affect plankton and micro-invertebrates living at the bottom of such water bodies. While the main toxic and volatile components of oil can be eliminated by evaporation, other components can be oxidized by the action of UV radiation from sunlight. Such compositional changes may modify the oil physical properties and toxicology. Furthermore, depending on the molecular weight, some oil components may deposit as sediment [1, 2].

Several strategies have been developed to reduce the impact of oil spills into the environment. For example, some biological methods use plants and microorganisms to degrade the oil, while chemical techniques use chemical agents to this end. Electrochemical methods, on the other side, can directly apply electrical energy to aid the remediation. They offer a broad spectrum of electrolytes and electrodes, and can be combined with biological agents as well as with ionic liquids [2-4].

Ionic liquids have been successfully implemented in diverse scientific/industrial areas such as catalysis, chemical synthesis, metals extraction, energy storage, supported liquid membranes, lubrication industry, production industry, solvents industry and pharmaceuticals. The diverse and extraordinary properties of ionic liquids can be adapted to the requirements of every application by the selection of an appropriate anion/cation combination. Ionic-liquid cations have normally an aromatic nature with nitrogen atoms within the aromatic ring, nitrogenated heterocycles, while the anionic part can be constituted by a variety of chemical elements. The cation is the main responsible of the molecule chemical behavior while the anion is the main responsible of the molecule physical characteristics. Among the different ionic liquids, the imidazolium-based ones have attracted great attention lately due to their thermal stability, high ionic conductivity and wide electrochemical window. Thus, they have a broad spectrum of promising applications [3-7].

Interest, has grown recently in studying the interaction of ionic liquids with diverse substances, and the subsequent modification of their properties [5-8]. Published studies deal with drugs [9], biomacromolecules [10], DNA of different animals such as veil [11-13], ferrocene-derived molecules [14], macrocyclic molecules such as Curcubit (6) Urile [15], etc. The studies range from computational modeling, such as molecular dynamics, to experimental methods including electrochemical techniques. In the latter case, interaction parameters such as the binding constant, the binding free energy and the diffusion coefficient of the ionic-liquid-bound molecule can be derived [16-18]. Additionally, for aqueous systems, the determination of the critical micelle concentration (CMC) becomes of great value. The CMC is the concentration at which the solution reaches saturation and thus the solute molecules aggregate into micelles. Above this point, significant changes in the physicochemical properties of the solution take place. The CMC provides important information on the ionic liquid surface activity [16-19]. The present work studies the interaction of an imidazole-based ionic liquid with light crude oil in a 70/30 oil/water emulsion by cyclic voltammetry. The ionic-liquid-to-oil binding-constant and binding-free-energy, as well as the diffusion coefficient of the free and bound forms of the oil within the emulsion are there from calculated. The applied methodology and derived data can be helpful to design new routes for the remediation of crude oil spilled into water bodies.

2. EXPERIMENTAL

2.1. Ionic Liquid synthesis

Figure 1 shows the synthesis route of the 1-methyl-3-hexylimidazolium p-toluenesulfonate ionic liquid. 1-methyl-3-hexylimidazolium bromide (synthesized as well at our laboratory) and sodium p-toluenesulfonate (Sigma Aldrich, 95% purity) were the anion-interchange-reaction precursors. Distilled water was used as reaction medium. The chemical synthesis was conducted during 24 h at 60°C under constant stirring. Afterwards, several evaporation and filtration cycles were used to eliminate, respectively, the remaining water and sodium bromide salt. The molecular structure of the synthesized ionic liquid was confirmed by Fourier-Transform Infrared Spectroscopy (FTIR) using a Perkin Elmer Spectrum 100 and by Nuclear Magnetic Resonance (NMR) using the Bruker Avance III HD 400 [18, 19].

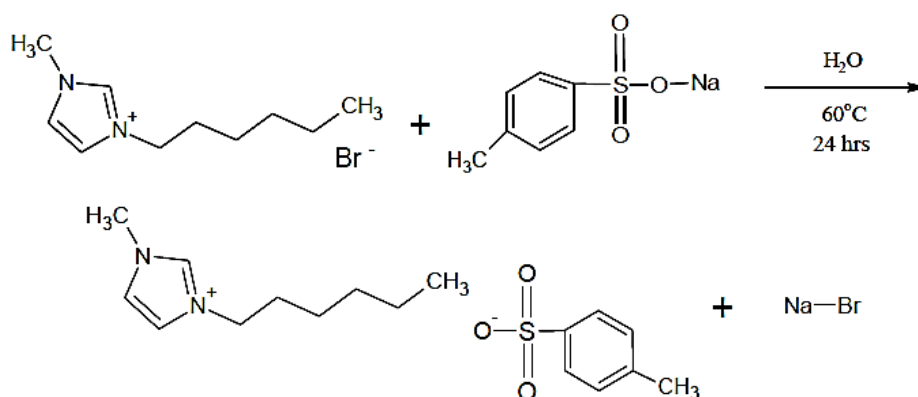


Figure 1. Synthesis route of 1-methyl-3-hexylimidazolium p-toluenesulfonate ionic liquid by anion interchange reaction of 1-methyl-3-hexylimidazolium bromide and sodium p-toluenesulfonate

2.2. Oil/Water Emulsion Preparation

The crude oil was extracted from the Aragon oil-well located within the Chicontepec region in central Mexico. The oil, characterized by the SARA analysis method, consists of 24% saturated hydrocarbons, 41% aromatic hydrocarbons, 34% resins and 0.8% asphaltenes. It has a density of 0.903 g/cm³ and a viscosity of 17.4 cP. The 70/30 oil/water emulsions were prepared with deionized water under constant stirring (4000 RPM, 5 minutes). Whenever required, the ionic liquid was added at the end of the stirring period [20-22].

2.3. Ionic Liquid Critical Micelle Concentration (CMC) in Water

The CMC of the ionic liquid in water was determined by three different techniques. First, by conductimetry using a HM Digital EC-3 conductimeter [23-25]. Afterwards by Ultraviolet-Visible Spectroscopy, using an Agilent Cary 60 spectrophotometer [25-30]. Finally by cyclic voltammetry using a BASi 100 B/W Potentiostat and a conventional 3-electrode cell with a silver wire as reference

electrode, a 304 stainless-steel plate (2.3 cm²) as counter electrode and a 304 stainless-steel perforated plate (1.7 cm²) as working electrode. Cyclic voltammograms were acquired scanning the potential from -1.2 V to +1.3 V at 0.8 V/s [31-35]. Twenty different concentrations of ionic-liquid aqueous-solutions in deionized water were tested (10 to 200 mg/L at 10 mg/L increments).

2.4. Diffusion Coefficient of the Free and Bound Crude-Oil

A conventional 3-electrode cell was used along with a silver wire as reference electrode, a 304 stainless-steel plate (2.3 cm²) as counter electrode and a 304 stainless-steel perforated plate (1.7 cm²) as working electrode. Cyclic voltammograms were acquired scanning the potential from -1.3 V to +1.3 V with scan rates ranging from 0.1 to 0.8 V/s. The diffusion coefficient was determined from the anodic peak-current (I_{pa}) by means of the Randles-Sevcik equation:

$$I_{pa} = 0.4463(nF)^{3/2}SC_oD^{1/2}\nu^{1/2}(RT)^{-1/2} \quad (1) [36]$$

where n is the number of transferred electrons, F is the Faraday constant, S is the electrode area (cm²), C_o is the reacting species bulk-concentration (mol/cm³), ν is the potential scan rate (V/s), R is the universal gas constant (J/mol K), T is the absolute temperature(K) and D is the diffusion coefficient (cm²/s). Plotting I_{pa} vs $\nu^{1/2}$ leads to a straight line whose slope m is related to D as follows:

$$D = \left(\frac{m}{0.4463(nF)^{3/2}SC_o(RT)^{-1/2}} \right)^2 \quad (2) [36-40]$$

2.5. Ionic-Liquid-to-Oil Binding-Constant and Binding-Free-Energy (70/30 Oil/Water Emulsion).

Cyclic voltammograms of oil/water emulsions, with ionic liquid in concentrations ranging from 10 to 150 mg/L, were acquired. The potential was scanned from -1.3 V to +1.3 V at a rate of 0.5 V/s, using a conventional 3-electrode cell with a silver wire as reference electrode, a 304 stainless-steel plate (2.3 cm²) as counter electrode and a 304 stainless-steel perforated plate (1.7 cm²) as working electrode. The decrease in anodic peak-current caused by the ionic liquid concentration increase followed Equation 3:

$$\frac{1}{C_{LI}} = \frac{K}{1 - \frac{i}{i_0}} - K \quad (3) [36-38]$$

where C_{LI} is the ionic liquid concentration in the oil/water emulsion (mol/L), K is the ionic-liquid-to-oil binding constant (L/mol), i_0 and i are the anodic peak current density (A/cm²) of the oil oxidation in the absence and presence, respectively, of ionic liquid. The calculated binding constant was used along with Equation 4 to determine the binding-free-energy (ΔG):

$$\Delta G = -RT \ln K \quad (4) [36, 37, 39-46]$$

3. RESULTS AND DISCUSSION

3.1. Ionic Liquid Synthesis

Figure 2 shows the FTIR spectrum of the synthesized ionic liquid. The 3377 and 567 cm^{-1} bands are due to the N-H bond stretching mode; the 2960, 2915 and 817 cm^{-1} bands are characteristic of the C-H bonds stretching mode; the 1653 cm^{-1} band is characteristic of the C=C groups stretching mode; the 1182 cm^{-1} band is characteristic of the C-N bonds; the 1182 and 1037 cm^{-1} bands are characteristic of the C-N and S=O bonds, respectively.

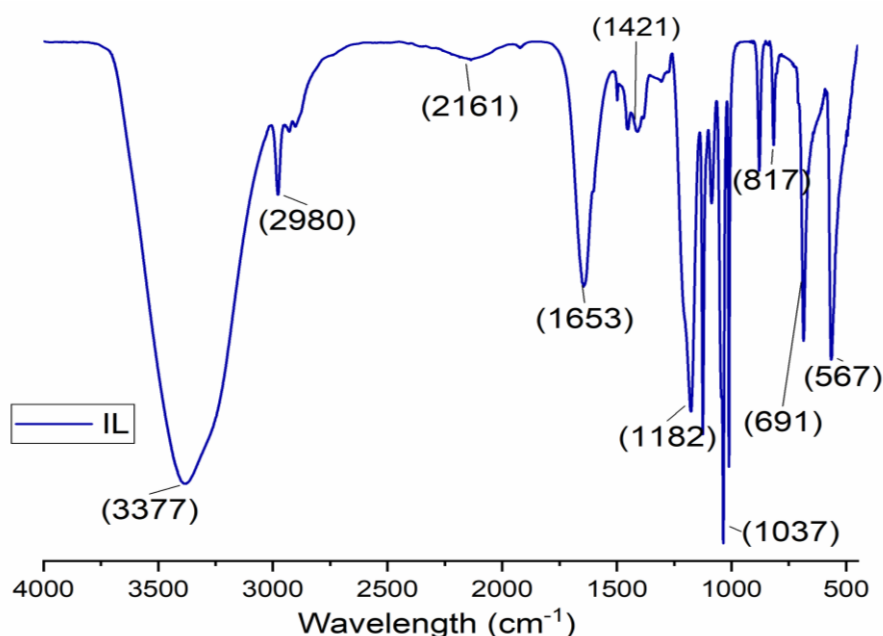


Figure 2. Fourier Transform Infrared spectrum of the synthesized 1-methyl-3-hexylimidazolium p-toluenesulfonate ionic-liquid.

Figure 3a shows the proton NMR spectrum of the synthesized ionic liquid. The following chemical shifts were there from identified: $-\text{CH}=\text{CH}$ -aromatic (7.58 ppm, doublet, 2H), $=\text{CH}-\text{NR}_2$ aromatic (7.36 ppm, doublet, 2H), $-\text{CH}=\text{CH}$ - aromatic (6.84 ppm, doublet, 2H), $-\text{CH}_2-\text{N}+\text{R}_3$ (4.37 ppm, triplet, 2H), CH_3-NR_2 (3.66 ppm, singlet, 3H), $\text{CH}_3-(\text{C}_6\text{H}_4)-$ (2.27 ppm, singlet, 3H), $-\text{CH}_2-\text{CH}_2-\text{N}+\text{R}_3$ (2.384 ppm, quintet, 2H), $-\text{CH}_2-\text{CH}_2\text{R}$ (1.96 ppm, quintet, 6H) y $\text{CH}_3-\text{CH}_2\text{R}$ (0.78 ppm, triplet, 3H). The carbon-13 RMN spectrum of the synthesized ionic liquid is observed in Figure 3b. The following chemical shifts were there from identified: $-\text{CH}=\text{CH}$ - aromatic (142.43, 140.14, 129.34 y 125.65 ppm), $-\text{CH}=\text{N}+\text{R}_2$ aromatic (136.84 ppm), $=\text{CH}-\text{NR}_2$ aromatic (122.41 ppm), $-\text{CH}_2-\text{N}+\text{R}_3$ (58.49 ppm), CH_3-NR_2 (36.08 ppm), $-\text{CH}_2-\text{CH}_2-$ (25.37 ppm), $-\text{CH}_2-\text{CH}_3$ (22.10 ppm), $\text{CH}_3-(\text{C}_6\text{H}_4)-$ (18.87 ppm) y $\text{CH}_3-\text{CH}_2\text{R}$ (0 y 0.80 ppm). Both the FTIR and NMR spectra characteristics confirmed the desired ionic-liquid molecular-structure was achieved with the implemented chemical synthesis procedure [18, 19].

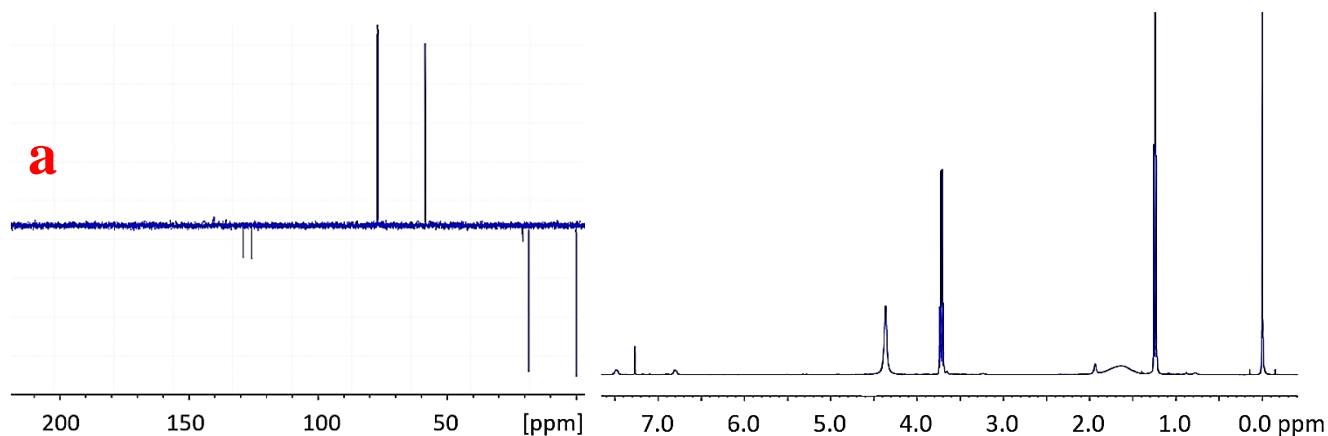


Figure 3. Nuclear Magnetic Resonance spectra of the synthesized 1-methyl-3-hexylimidazolium p-toluenesulfonate ionic-liquid a) proton spectrum, b) carbon-13 spectrum.

3.2. Determination of the Ionic Liquid Critical Micelle Concentration (CMC) in Water

The conductimetry technique results can be observed in Figure 4. The ionic conductivity of the solution increases linearly with ionic liquid concentration from 10 to 152 mg/L. Afterwards, the linear behavior changes abruptly.

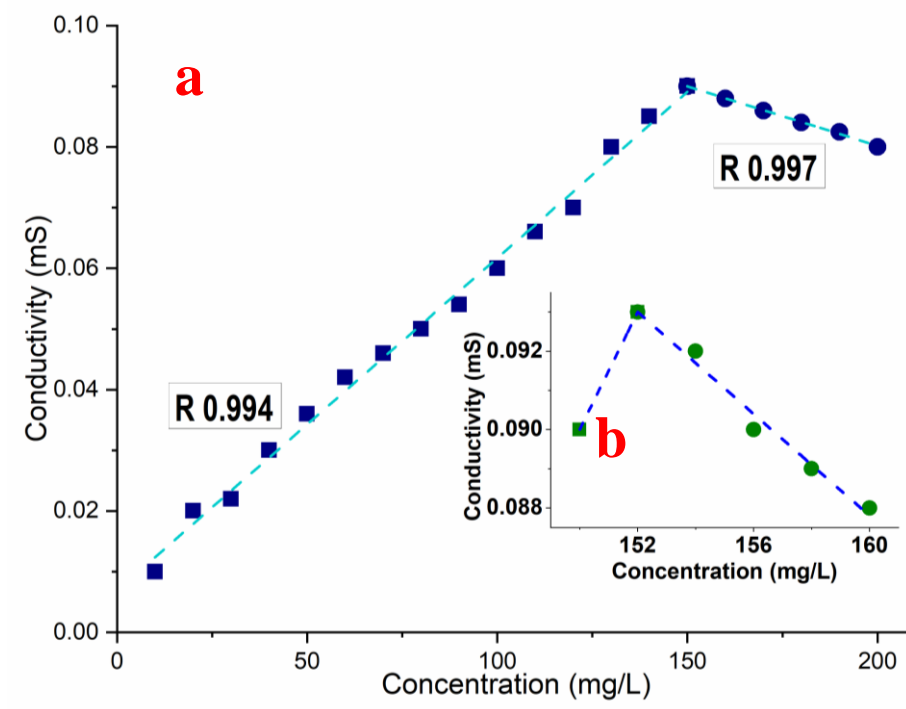


Figure 4. Determination of the Critical Micelle Concentration of 1-methyl-3-hexylimidazolium p-toluenesulfonate ionic liquid in water by Conductimetry: a) 10 to 200 mg/L ionic liquid concentration range, b) 150 to 160 mg/L ionic liquid concentration range.

The inflection point is associated with the CMC, as reported in the literature [23]. It represents

the initiation of micellization. For the pre and post-micellar regions, a linear regression coefficient of, respectively, 0.994 and 0.997 was obtained. This indicates the ionic liquid is a normal surfactant with a clear CMC [24]. The decrease in solution ionic conductivity after the CMC can be ascribed to the incorporation of ionic liquid molecules into the micellar structures which have a larger molecular weight and thus are less mobile [25].

Figure 5a shows the UV-Vis absorption spectrum of the 100 mg/L solution of 1-methyl-3-hexylimidazolium p-toluenesulfonate ionic liquid in water. Figure 5b shows the variation of the main-absorption-peak height (200 to 260 nm wavelength interval) with ionic liquid concentration from 10 to 200 mg/L. The CMC can be determined from the observed peak behavior [27]. As shown in Figures 6a and 6b, below the CMC the peak absorbance increases continuously along with ionic liquid concentration. This is attributed to the presence of imidazolium-ion aggregates. The absorbance follows the Lambert-Beer law, i.e. it is proportional to the concentration of absorbing species. Close to the CMC, however, there is an inflection point. Such absorption behavior is typical of imidazolium based ionic liquids. At concentrations above 150 mg/L the peak absorbance decreases due to the micellar saturation process [27]. According to Figure 6b, the CMC can be found at around 154 mg/L [27, 28].

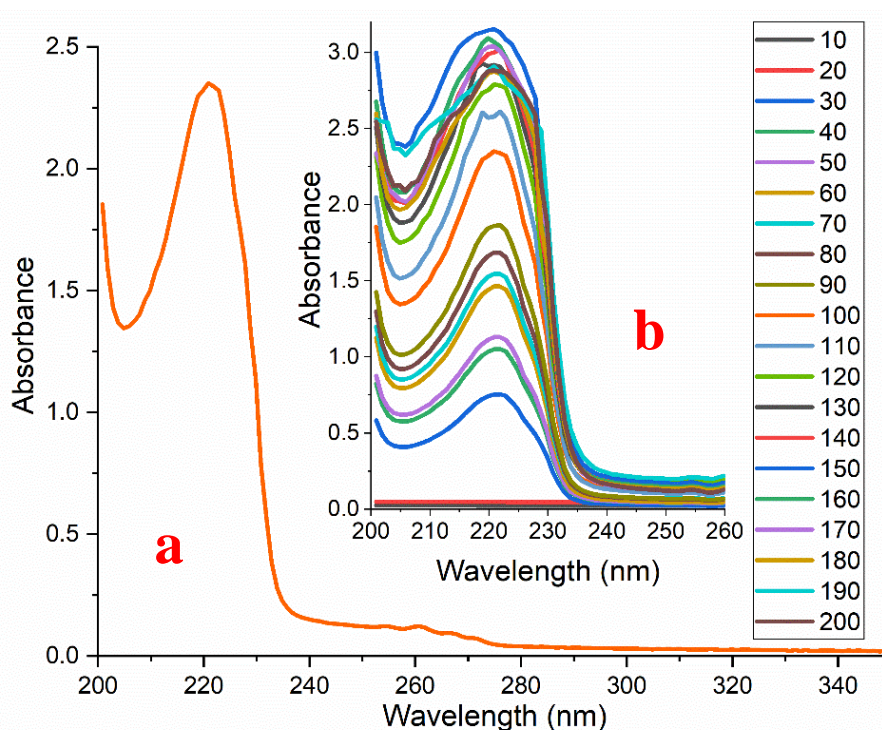


Figure 5. UV-Vis spectra of 1-methyl-3-hexylimidazolium p-toluenesulfonate ionic liquid in water: a) 100 mg/L ionic liquid concentration, b) 10 to 200 mg/L ionic-liquid concentration range.

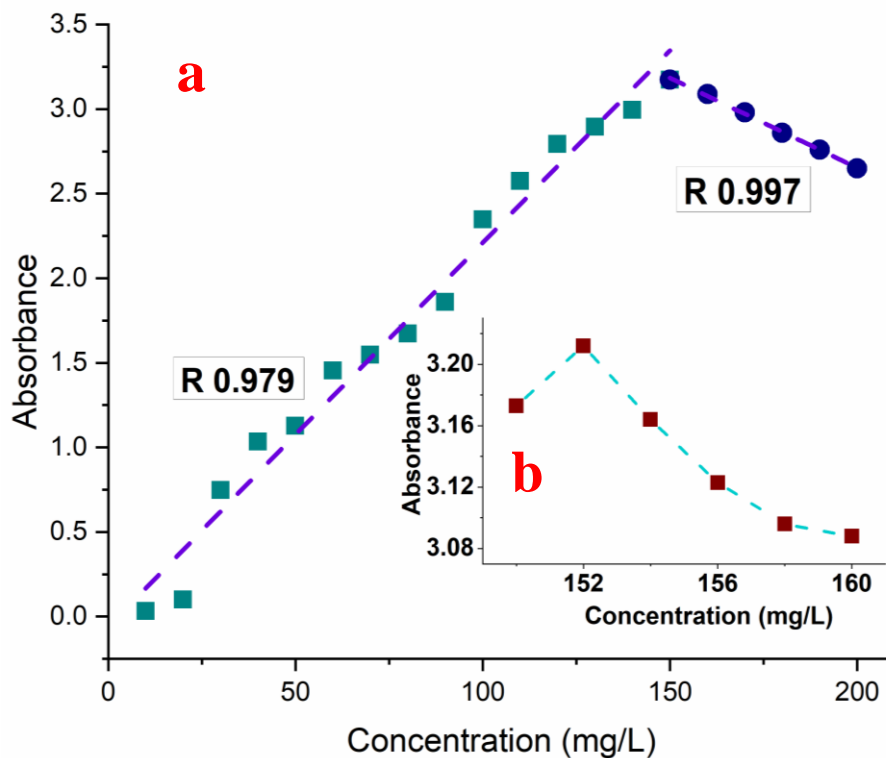


Figure 6. Determination of the Critical Micelle Concentration of 1-methyl-3-hexylimidazolium p-toluenesulfonate ionic liquid in water by UV-Vis spectroscopy (main absorption peak height): a) 10 to 200 mg/L ionic-liquid concentration range, b) 150 to 160 mg/L ionic liquid concentration range.

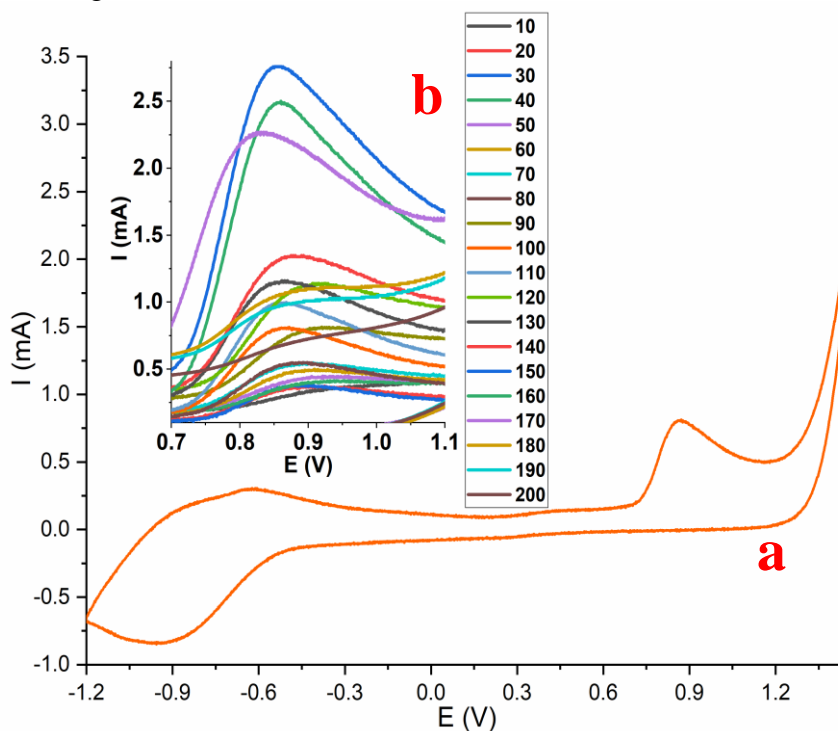


Figure 7. Cyclic voltammograms of 1-methyl-3-hexylimidazolium p-toluenesulfonate ionic liquid in water (scan rate:0.8 V/s, reference electrode: silver wire, working electrode and counter electrode: 304 stainless-steel plate): a) 100 mg/L ionic liquid concentration, b) 10 to 200 mg/L ionic liquid concentration range.

Figure 7a shows the cyclic voltammogram of the 100 mg/L ionic liquid aqueous solution. The oxidation and reduction peaks of the ionic-liquid electroactive-units can be observed. Figure 7b shows the variation of the anodic-peak (at around 900 mV) with ionic liquid concentration. The anodic peak corresponds to the electron transfer from anion to cation within the ionic liquid molecule, due to the high electron density of the former.

Figure 8a plots the anodic peak-current as a function of ionic liquid concentration in the 10 to 200 mg/L range. The peak current increases with concentration up to 152 mg/L (Figure 8b), where an inflection point is observed. Afterwards, the peak current goes down. The peak current is a function of both the concentration and the diffusion coefficient of reacting species. Thus, beyond the CMC, the current behavior stems from a smaller amount of free ionic liquid units present in solution and the lower diffusion coefficient that the newly-formed micelles have. In this way, the CMC was found to be around 152 mg/L [31, 32, 35].

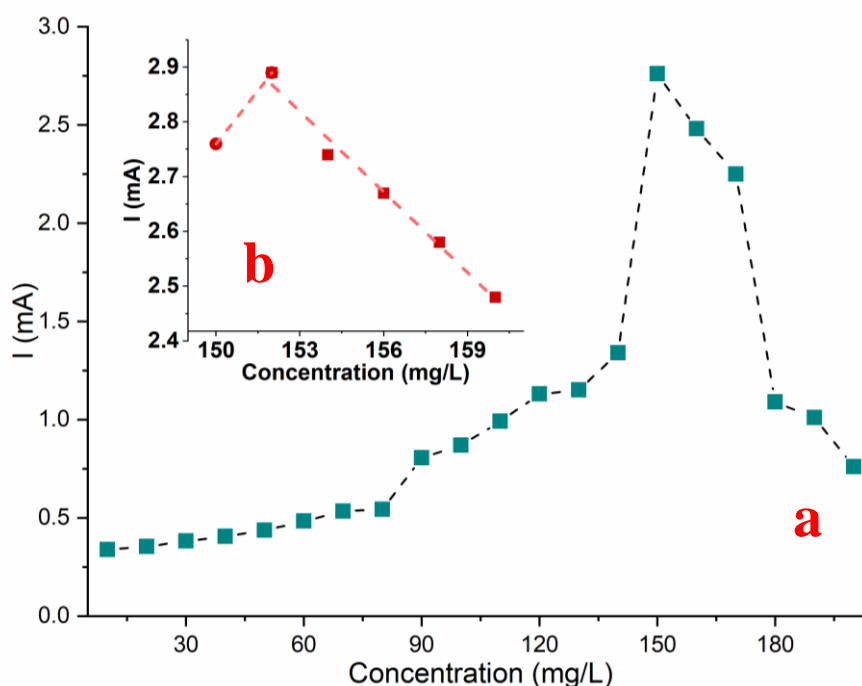


Figure 8. Determination of the Critical-Micelle-Concentration of 1-methyl-3-hexylimidazolium p-toluenesulfonate ionic liquid in water by cyclic voltammetry (anodic peak-current): a) 10 to 200 mg/L ionic-liquid concentration range, b) 150 to 160 mg/L ionic liquid concentration range.

An average CMC value of 152.6 mg/L for the 1-methyl-3-hexylimidazolium p-toluenesulfonate ionic liquid was calculated from the results of three different techniques used to determine such parameter.

3.3. Diffusion Coefficient of the Free and Bound Crude-Oil

Figure 9a, shows the cyclic voltammograms of oil/water emulsion acquired at the 8 different scan rates tested. Several redox processes associated with the Aragon crude-oil are observed. A major anodic peak appears at around -0.2 V and, afterwards, the current increases due to decomposition of the medium. Such processes are shifted to more negative values by adding ionic liquid to the system (figure 9b). A quasi-reversible signal is then observed at a half-wave potential of -0.45 V, with larger associated currents at each scan rate. The anodic peak-current of the system with and without ionic liquid is plotted vs. the square root of the scan rate in Figure 10. Applying Equation 2 to the slope of the data linear fit leads to a diffusion coefficient of $D = 1.852 \times 10^{-7} \text{ cm}^2/\text{s}$ for the water/oil system, and $D = 4.631 \times 10^{-7} \text{ cm}^2/\text{s}$ for the ionic-liquid modified system. An approximate 2.5-fold increase in the oil diffusion coefficient was thus achieved by adding the ionic liquid [36-40].

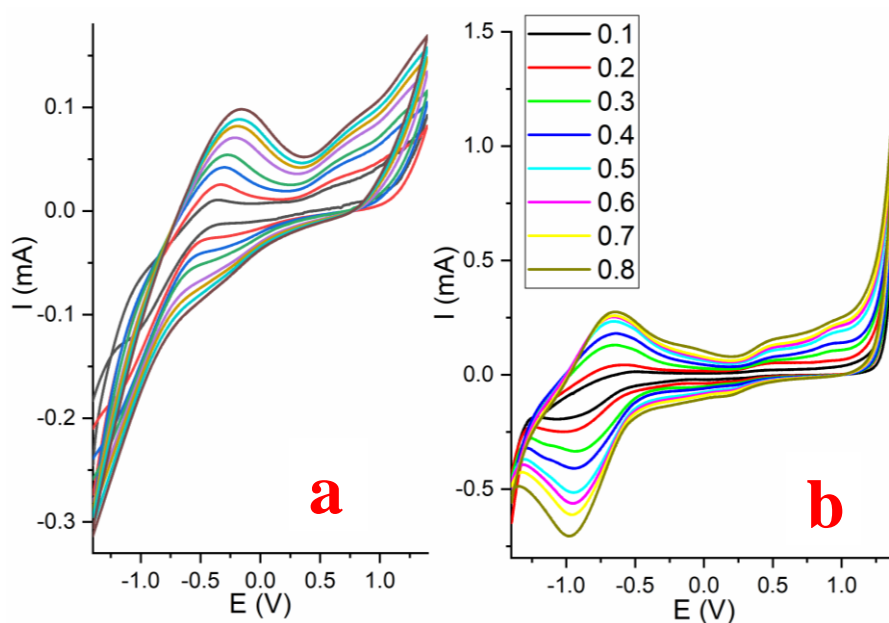


Figure 9. Cyclic voltammograms of a) 70/30 Aragon-oil/water emulsion, b) 70/30 Aragon-oil/water emulsion + 1-methyl-3-hexylimidazolium p-toluenesulfonate ionic liquid (150 mg/L). Scan rate range: 0.1 to 0.8 V/s, reference electrode: silver wire, working electrode and counter electrode: 304 stainless-steel plate.

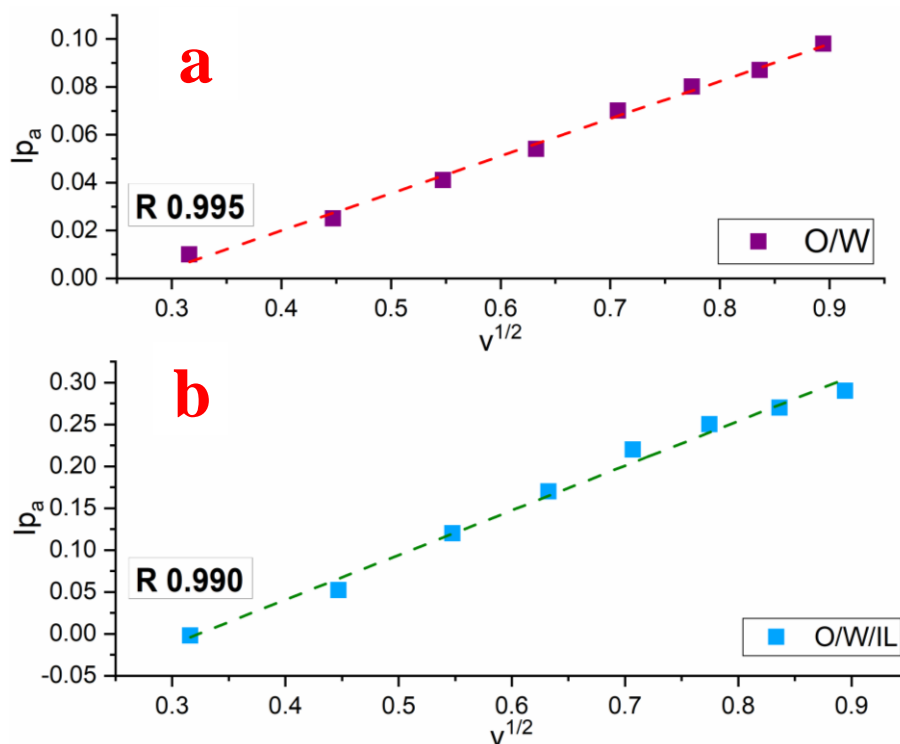


Figure 10. Anodic peak-current versus cyclic-voltammogram scan rate for the determination of the diffusion coefficient via the Randles-Sevcik Equation (Equation 1) of Aragon-oil in: a) 70/30 oil/water emulsion, b) 70/30 oil/water emulsion + 1-methyl-3-hexylimidazolium p-toluenesulfonate ionic liquid (150 mg/L).

3.4. Binding Constant and Binding Free Energy

Figure 11a shows the cyclic voltammogram of the 70/30 oil/water/ionic-liquid emulsion (70 mg/L). A major anodic peak is observed at around -0.7 V. Figure 11b shows the anodic peak decrease with increasing ionic liquid concentration in the emulsion.

Figure 12 shows the I/C_{LI} vs. $I/(1-i/i_0)$ plot, together with the equation of the best linear fit attained, and its corresponding correlation coefficient (R^2). Using Equation 3, a binding constant (K) of 0.98×10^4 L/mol is determined [41-43]. Such K corresponds to a binding free-energy of -22.78 KJ/mol (Equation 4). The free-energy negative value is an indicator of the spontaneous nature of the interaction [38-42]. Such observations are common to systems where ionic liquids are involved, due to their ionic properties which that favor migration and species-interchange phenomena.

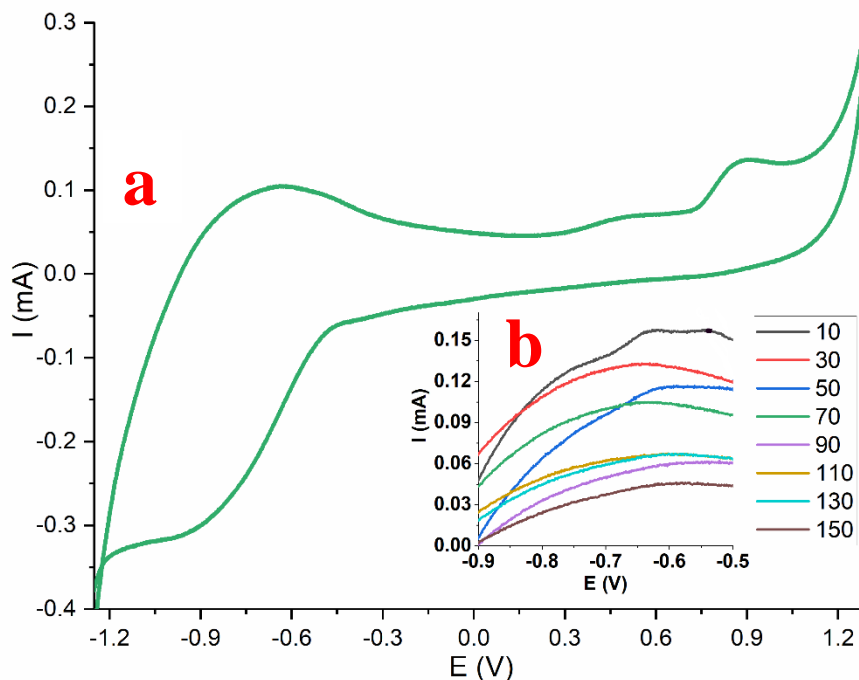


Figure 11. Cyclic voltammograms (scan rate: 0.5 V/s, reference electrode: silver wire, working electrode and counter electrode: 304 stainless-steel plate) of the 70/30 Aragon-oil/water emulsion +1-methyl-3-hexylimidazolium p-toluenesulfonate ionic liquid: a)70 mg/L ionic liquid, b)10 to 150 mg/Lionic liquid concentration range.

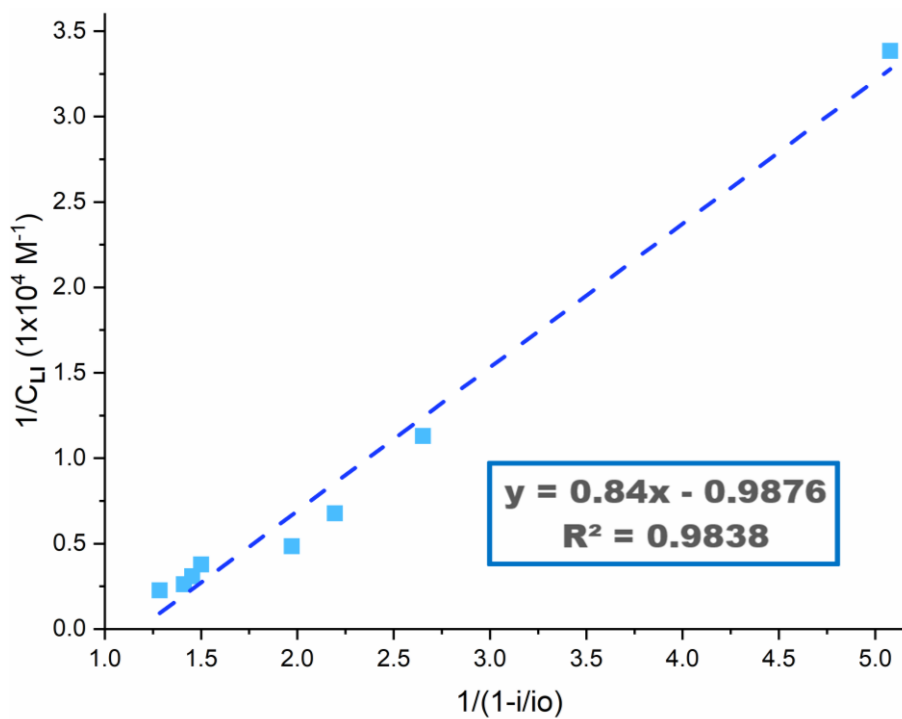


Figure 12. Determination of the binding constant of 70/30 Aragon-oil/water emulsion +1-methyl-3-hexylimidazolium p-toluenesulfonate ionic liquid (10 to 150 mg/L) from the cyclic-voltammograms anodic-peak-current via Equation 3.

4. CONCLUSIONS

The ionic liquid synthesis procedure was successful and the desired molecular structure was achieved, as proved by the FTIR and NMR acquired spectra. The CMC determination can be adequately conducted by any of the techniques hereby tested. Cyclic Voltammetry confirmed the existence of a convenient interaction between the ionic liquid and the oil in the oil/water emulsion. The diffusion coefficient of the oil was enhanced with the addition of ionic liquid. The binding constant resulted negative and the Gibbs free energy indicates the spontaneous nature of the binding process.

ACKNOWLEDGMENTS

E.E. Villalobos-Neri acknowledges the scholarship provided by CONACYT-Mexico. The authors would like to thank Consejo Nacional de Ciencia y Tecnología (CONACYT-México) Projects of Scientific Development to Address National Problems (APN-No.3676) and Tecnológico Nacional de México (TecNM) for financial support.

References

1. I. C. Ossai, A. Ahmed, A. Hassan, and F. S. Hamid, *Environ. Technol. Innov.*, 17 (2020) 100526.
2. S. Kuppusamy, N. R. Maddela, M. Megharaj, and K. Venkateswarlu, *Total petroleum hydrocarbons: Environmental Fate, Toxicity and Remediation*, (2019) Springer Cham, Switzerland.
3. M. J. Earle and K. R. Seddon, *Pure Appl. Chem.*, 72 (2020) 1391.
4. M. K. Banjare, K. Behera, R. K. Banjare, S. Pandey, and K. K. Ghosh, *J. Mol. Liq.*, 302 (2020) 112530.
5. J. G. Huddleston, A. E. Visser, W. M. Reichert, H. D. Willauer, G. A. Broker, and R. D. Rogers, *Green Chem.*, 3 (2001) 156.
6. K. Behera and S. Pandey, *J. Colloid Interface Sci.*, 331 (2009) 196.
7. J. Bowers, C. P. Butts, P. J. Martin, M. C. Vergara-Gutierrez, and R. K. Heenan, *Langmuir*, 20 (2004) 2191.
8. C. J. Moreira, A. Bento, J. Pais, J. Petit, R. Escórcio, V. G. Correia, and C. S. Pereira, *Plant Physiol.*, 184(2020) 592.
9. H. Kumar, and P. Sharma, *J. Phys.: Conference Series*, 1531 (2020) 012104.
10. J. J. Xue, and Q. Y. Chen, *Spectrochim. Acta A Mol. Biomol. Spectrosc.*, 120 (2014) 161.
11. M. H. Nasir, E. Jabeen, R. Qureshi, F. L. Ansari, A. Shaukat, U. Nasir, and A. Ahmed, *Biophys. Chem.*, 258 (2020) 106316.
12. K. Jumbri, M. A. Kassim, N. Yunus, M. B. Abdul Rahman, H. Ahmad, and R. Abdul Wahab, *Processes*, 8 (2020) 13.
13. N. K. Janjua, Z. Akhter, F. Jabeen, and B. Iftikhar, *J. Korean Chem. Soc.*, 58 (2014) 153.
14. M. Pešić, J. Bugarinović, A. Minić, S. B. Novaković, G. A. Bogdanović, A. Todosijević, and I. Damljanović, *Bioelectrochem.*, 132 (2020) 107412.
15. Z. Miskolczy, L. Biczók, M. Megyesi, and I. Jablonkai, *J. Phys. Chem. B*, 113(2009) 1645.
16. C. Jungnickel, J. Łuczak, J. Ranke, J. F. Fernández, A. Müller, and J. Thöming, *Colloids Surf. A Physicochem. Eng. Asp.*, 316 (2008) 278.
17. M. Blesic, M. H. Marques, N. V. Plechkova, K. R. Seddon, L. P. N. Rebelo, and A. Lopes, *Green Chem.*, 9(2007) 481.
18. M. S. Googheri, M. S. S., Googheri, and S. H. Araghi, *J. Molec. Liq.*, 263 (2018) 158.
19. D. Zhao, Z. Fei, R. Scopelliti, and P. J. Dyson, *Inorg. Chem.*, 43 (2004) 2197.
20. K. C. Powell, R. Damitz, and A. Chauhan, *Int. J. Pharm.*, 521(2017) 8.

21. J. Zhang, D. Huang, G. Wu, S. C. Chen, and Y. Z. Wang, *J. Hazard. Mater.*, 400 (2020) 123132.
22. Z. Derikvand, A. Rezaei, R. Parsaei, M. Riazi, and F. Torabi, *Colloids Surf. A Physicochem. Eng. Asp.*, 587 (2020) 124327.
23. S. Chauhan, and K. Sharma, *J. Chem. Thermodyn.*, 71 (2014) 205.
24. S. Sharma, K. Kumar, and S. Chauhan, *J. Molec. Liq.*, 300 (2020) 112306.
25. N. Scholz, T. Behnke, and U. Resch-Genger, *J. Fluoresc.*, 28 (2018) 465.
26. T. Nasiru, L. Avila, and M. Levine, *J. High Sch. Res.*, 2 (2011) 1.
27. J. Fu, Z. Cai, Y. Gong, S. E. O'Reilly, X. Hao, and D. Zhao, *Colloids Surf. A: Physicochem, Eng. Asp.*, 484 (2015) 1.
28. M. A. Hoque, S. Mahbub, M. D. Hossain, M. A. Khan, J. M. Khan, A. Malik, and M. Z. Ahmed, *J. Molec. Liq.*, (2021) 115418.
29. Z. Wei, D. Yi, X. Hu, C. Sun, Y. Long, and H. Zheng, *Colloids Surf. A Physicochem. Eng. Asp.*, 595 (2020) 124698.
30. A. Beyaz, W. S. Oh, and V. P. Reddy, *Colloids Surf. B*, 35(2004) 119.
31. L. Aldous, D. S. Silvester, W. R. Pitner, R. G. Compton, M. C. Lagunas, and C. Hardacre, *J. Phys. Chem. C*, 111 (2007) 8496.
32. J. Zhang, and A. M. Bond, *Analyst*, 130 (2005) 1132.
33. K. Nesměrák, and I. Němcová, *Anal. Lett.*, 39 (2006) 1023.
34. Y. C. Ko, *Bull. Korean Chem. Soc.*, 28 (2007) 1857.
35. B. N. Viada, A. V. Juárez, E. M. P. Gómez, M. A. Fernández, and L. M. Yudi, *Electrochim. Acta*, 263 (2018) 499.
36. T. Lanez, M. Henni, and H. Hemmami, *Sci. Study Res. Chem. Chem. Eng. Biotechnol. Food Ind.*, 16 (2015) 161.
37. G. C. Zhao, J. J. Zhu, J. J. Zhang, and H. Y. Chen, *Anal. Chim. Acta*, 394(1999) 337.
38. S. Mahajan, R. Sharma, and R. K. Mahajan, *Langmuir*, 28(2012) 17238.
39. J. Gonzalez, F. Martinez-Ortiz, E. Torralba, and A. Molina, *Chem. Electrochem.*, 6 (2019) 473.
40. X. Hu, Q. Lin, J. Gao, Y. Wu, and Z. Zhang, *Chem. Phys. Lett.*, 516 (2011) 35.
41. L. Hu, H. Peng, Y. Zhang, Q. Xia, H. He, R. Ruan, and A. Liu, *Carbohydr. Polym.*, 231 (2020) 115699.
42. Y. N. Xie, S. F. Wang, Z. L. Zhang, and D. W. Pang, *J. Phys. Chem. B*, 112 (2008) 9864.
43. C. S. Pomelli, C. Chiappe, A. Vidis, G. Laurenczy, and P. J. Dyson, *J. Phys. Chem. B*, 111 (2007) 13014.
44. H. Wang, J. Wang, and S. Zhang, *Phys. Chem. Chem. Phys.*, 13 (2011) 3906.
45. N. Zhao, L. Liu, F. Biedermann, and O. A. Scherman, *Chem. Asian J.*, 5 (2010) 530.
46. J. Zhou, J. Mao, and S. Zhang, *Fuel Process. Technol.*, 89 (2008) 1456.